Statistical second-order two-scale analysis and computation for heat conduction problem with radiation boundary condition in porous materials*

Zhi-Qiang Yang(杨志强)†, Shi-Wei Liu(刘世伟), and Yi Sun(孙毅)

Department of Astronautic Science and Mechanics, Harbin Institute of Technology, Harbin 150001, *China*

(Received 21 February 2016; revised manuscript received 15 May 2016; published online 2 August 2016)

This paper discusses a statistical second-order two-scale (SSOTS) analysis and computation for a heat conduction problem with a radiation boundary condition in random porous materials. Firstly, the microscopic configuration for the structure with random distribution is briefly characterized. Secondly, the SSOTS formulae for computing the heat transfer problem are derived successively by means of the construction way for each cell. Then, the statistical prediction algorithm based on the proposed two-scale model is described in detail. Finally, some numerical experiments are proposed, which show that the SSOTS method developed in this paper is effective for predicting the heat transfer performance of porous materials and demonstrating its significant applications in actual engineering computation.

Keywords: statistical second-order two-scale method, radiation boundary condition, random porous materials

PACS: 02.30.Jr, 44.40.+a, 02.60.–x, 02.60.Cb **DOI:** 10.1088/1674-1056/25/9/090202

1. Introduction

Porous materials are of significance in engineering and industry on account of their high temperature resistance, corrosion resistance, fatigue resistance, and even in bio-medical engineering. In particular, as the rapid development of the aerospace industry, porous materials have drawn tremendous attention and wide research interest from scientists and engineers.[1–7] Inevitably, our attention is focused on predicting the effective macroscopic properties of porous materials.

Convection takes place by flow of fluids and can be ignored at low pressure or in porous materials with a closed cell structure.[1,2] Radiation is a way of heat transmission and plays a significant role in modern technology, especially as the temperature on a visible surface of the system is high enough. Some interesting work has been proposed to consider the surface radiation of porous materials in the past years. Liu and Zhang[1] gave the effective macroscopic thermal properties of the coupled conduction and radiation problem with a small parameter ε. Bakhvalov[3] introduced the asymptotic homogenization method for the solutions of those problems. Later, Cui *et al.*[4,5] investigated the coupled heat transfer problem with rapidly oscillating coefficients, and gave the theoretical verification. Allaire and Ganaoui[6] studied the coupled problem with non-linear interior surface radiation of porous materials by a two-scale homogenization method, and obtained the error estimates. Meanwhile, Ma and Cui[7] discussed a second-order multiscale analysis and computation for the heat transfer problem, and justified the convergence results with an explicit rate $\varepsilon^{1/2}$. In theory, some authors[8–11] gave detailed proofs of the existence and uniqueness of the heat conduction equation considering non-linear radiation boundary conditions.

Solving the heat conduction problem with a radiation boundary condition which arises in porous materials will be discussed in this study. Under such conditions, the direct finite element simulation in a very fine spatial mesh is necessary for porous materials to acquire the microscale effect, and thus a prohibitive amount of computation time and computer memory exceed the ability of a general computer. In this context, a homogenized method and the associated multiscale method, which are described in sources[12–16] and other references, are introduced. The basic idea of the homogenized method is to describe the macroscopic behavior of the porous materials by absorbing the local oscillation due to the inhomogeneity, which cannot only save the computational effort but also insure the accuracy. On the basis of the homogenization method, He and Cui *et al.* established an SSOTS analysis method to predict the physical and mechanical performance of the composite structure through introducing a random sample model.[17–21] However, the theoretical verification is not enough for the random composites.[20] Meanwhile, Jikov *et al.*[16] proved the existences of the homogenized coefficients and the homogenized solution for the randomly distributed composite. Yu *et al.*[19] developed a novel algorithm for generating the random unit cell, which is based on a probability distribution model of the grains (pores). Compared with other micromechanics methods, such as the Mori–Tanaka method,[22] the self-consistent method,[23] the generalized self-consistent method,[24] and the Maxwell–Eucken model,[25] the homogenized method has a rigorous mathematical background and it

*Project supported by the China Postdoctoral Science Foundation (Grant Nos. 2015M580256 and 2016T90276).

†Corresponding author. E-mail: yangzhiqiang@hit.edu.cn

© 2016 Chinese Physical Society and IOP Publishing Ltd

contains almost all the microcosmic information of the composites.

The main new results obtained in this paper are an approximate error analysis in pointwise sense for the SSOTS method and to develop an efficient prediction algorithm for solving the nonlinear heat transfer problem.

This rest of this paper is organized as follows. In Section 2, the microscopic configurations for porous materials with random distributions are represented. Section 3 is devoted to the SSOTS formulae for prediction of the thermal properties of the porous materials. In Section 4, numerical results for the heat transfer performance of porous materials are obtained from the proposed two-scale analysis. Finally, Section 5 is devoted to the conclusions.

2. Microscopic representation of porous materials with random distribution

The investigated porous materials are composed of a matrix and random pores. All the pores are considered as ellipsoids, which are randomly distributed in the matrix. Similarly to Refs. [18] and [19], the microstructure of porous materials with random distribution can be described in detail as follows.

1) In the investigated structure Ω^ε, there exists a constant ε satisfying $0 < \varepsilon \ll L$, where L denotes the macroscale structure of Ω^ε. Thus, Ω^ε is made from all the cells of size ε, as shown in Fig. 1(a).

2) Each ellipsoid is described in three-dimensional (3D) space by the shape, size, orientation, and spatial distribution of ellipsoid pores: a_1, a_2, a_3, β_1, β_2, β_3, x_{01}, x_{02}, x_{03}, where a_1, a_2, and a_3 denote the lengths of three axes; β_1, β_2, and β_3 are three Euler angles of the rotations; x_{01}, x_{02}, and x_{03} are the coordinates of the center. Let the random vector $\xi = (a_1, a_2, a_3, \beta_1, \beta_2, \beta_3, x_{01}, x_{02}, x_{03})$, which contains all the information of an ellipsoid.

3) Let a cell εY^s include K ellipsoids, where Y^s represents a normalized cell and $s = 1, 2, 3, \ldots$ denotes the index of samples. Then, the corresponding random sample ω^s of ellipsoidal distribution is defined as

$$\omega^s = (\xi_1^s, \xi_2^s, \xi_3^s, \ldots, \xi_{K-1}^s, \xi_K^s).$$

Therefore, the porous structure Ω^ε consists of ε-size cells subjected to identical probability distribution model P, part of which is shown in Fig. 1(b).

In the following, the thermal conductivity parameters of the porous materials can be considered by

$$\{k_{ij}^\varepsilon(x, \omega^s)\} = k_{ij}^1, \quad \text{if } x \in \varepsilon Y^s - \bigcup_{k=1}^{K} e_k,$$

where e_k denotes the kth ellipsoid inside εY^s; k_{ij}^1 represents the material coefficient of the matrix, and satisfies that $\left|k_{ij}^1\right| < \tilde{M}$, where $\tilde{M}$ is a positive constant.

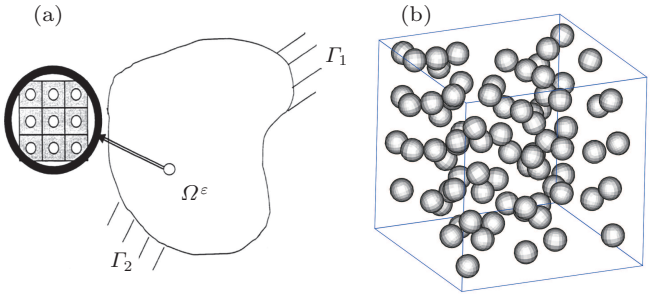


Fig. 1. Porous materials with random distribution of pores. (a) The whole structure Ω^ε and (b) unit cell Y^{*s}.

3. Second-order two-scale method

In this section, the SSOTS formulae are given for predicting effective properties of the heat transfer problem in detail, including expected homogenized parameters and the homogenized solution.

Let $Y = \{y : 0 \le y_j \le 1, j = 1, 2, 3\}$ and ϖ be an unbounded domain of R^3 which satisfies the conditions as follows.

(I) ϖ is a smooth unbounded domain of R^3 with a random structure.

(II) The unit cell $Y^* = \varpi \cap Y$ is a domain with a Lipschitz boundary. $\partial Y^* = \partial Y \cup \Gamma$, where Γ is the surfaces of cavities and Y^* is the solid part of Y, depicted in Fig. 1(b).

(III) The set $Y \backslash \bar{\varpi}$ and the intersection of set $Y \backslash \bar{\varpi}$ with the δ_0 distance of ∂Y consist of a finite number of Lipschitz domains separated from each other.

(IV) The cavities of the domain are convex.

Then, the investigated porous domain Ω^ε as shown in Fig. 1(a) has the form: $\Omega^\varepsilon = \Omega \cap \varepsilon\varpi$ and $\partial\Omega^\varepsilon = \partial\Omega \cup \Gamma_\varepsilon^c$, where Ω is a bounded convex domain of R^3 without cavities, and the cavities do not intersect. The Γ_ε^c is the domain made from interior surfaces of $\Gamma_{\varepsilon,m}^c$, such that $\Gamma_\varepsilon^c = \bigcup_{m=1}^{m(\varepsilon)} \Gamma_{\varepsilon,m}^c$, and $m(\varepsilon)$ is the number of cavities contained in the porous materials.

The nonlinear heat transfer problem is firstly investigated by Bakhvalov,[3] and later by Liu and Zhang[1] and Cui *et al.*,[4,5,26] in which the radiation in an interior surface of a closed cavity is defined by

$$-\nu_i k_{ij}^\varepsilon(x, \omega) \frac{\partial T_\varepsilon(x, \omega)}{\partial x_j} = e\sigma T_\varepsilon^4(x, \omega) - e \int_{\Gamma_{\varepsilon,m}^c} R_\varepsilon(x, \omega) F(x, z)\, \mathrm{d}z,$$

where $T_\varepsilon(x, \omega)$ denotes the temperature; σ is the Stefan–Boltzmann constant; $\nu = (\nu_i)$ $(i = 1, 2, 3)$ is the unit outward normal on Γ_ε. The emissivity e, which satisfies $0 < e \le 1$, $R_\varepsilon(x, \omega)$ is the intensity of emitted radiation given by

$$R_\varepsilon(x, \omega) = e\sigma T_\varepsilon^4(x, \omega) + (1 - e) \int_{\Gamma_{\varepsilon,m}^c} R_\varepsilon(z, \omega) F(x, z)\, \mathrm{d}z, \quad \forall x \in \Gamma_{\varepsilon,m}^c.$$

For any fixed sample ω, similarly to the proof obtained by Yang *et al.*,[4,5] $R_\varepsilon(x,\omega)$ has the unique solution. Furthermore, we assume that the surfaces of cavities are diffuse and grey, and the gas inside the cavities is supposed to be transparent.

Thus, under the aforementioned assumptions, the mixed boundary value problem of a heat conduction problem with radiation boundary condition can be expressed as follows:

$$\begin{cases} -\dfrac{\partial}{\partial x_i}\left[k_{ij}^{\varepsilon}(x,\omega)\dfrac{\partial T_\varepsilon(x,\omega)}{\partial x_j}\right]=f(x), & x\in\Omega^{\varepsilon},\\ T_\varepsilon(x,\omega)=\bar{T}(x), & x\in\Gamma_1,\\ \nu_i k_{ij}^{\varepsilon}(x,\omega)\dfrac{\partial T_\varepsilon(x,\omega)}{\partial x_j}=0, & x\in\Gamma_2,\\ -\nu_i k_{ij}^{\varepsilon}(x,\omega)\dfrac{\partial T_\varepsilon(x,\omega)}{\partial x_j}\\ =e\sigma T_\varepsilon^4(x,\omega)-e\int_{\Gamma_{\varepsilon,m}^c}R_\varepsilon(x,\omega)F(x,z)\,\mathrm{d}z, & x\in\Gamma_\varepsilon^c, \end{cases} \tag{1}$$

where $k_{ij}^{\varepsilon}(x,\omega)$ $(i,j=1,2,3)$ is the coefficient of the thermal conductivity, and $\bar{T}(x)$ is the boundary temperature on Γ_1. The Γ_2 is the boundary where heat flux is specified, and satisfies $\Gamma_1\cup\Gamma_2=\partial\Omega$, $\Gamma_1\cap\Gamma_2=\emptyset$. The $F(x,z)$ is the view factor defined on 3D form for a convex cavity as follows:[4–7,10,11]

$$F(x,z)=\frac{n_z(x-z)n_x(z-x)}{\pi|z-x|^4},$$

where n_z and n_x denote the unit normal at the different points z and x on $\Gamma_{\varepsilon,m}^c$, respectively.

In the following, we suppose that

(i) If $\{k(\omega)\}$ is a bounded random variable, and there exists an expectation value.

(ii) $\{k_{ij}(x/\varepsilon,\omega)\}$ is symmetric and bounded, that is, there exist two positive constants c_1 and c_2 such that

$$c_1\eta_i\eta_i\le k_{ij}\left(\frac{x}{\varepsilon},\omega\right)\eta_i\eta_j\le c_2\eta_j\eta_j.$$

Remark 1 By suppositions (I)–(IV), (i) and (ii), for any fixed sample $\omega\in P$, the boundary value problem (1) has the unique weak solution $T_\varepsilon(x,\omega)$.[10,11]

It is well known that the temperature increments of porous materials with random distribution not only depend on the macroscopic behaviors, but also on microscopic configurations; hence it can be expressed as $T_\varepsilon(x,\omega)=T(x,y,\omega)$, where $y=x/\varepsilon$, x denotes the macroscopic coordinate and y is the local one. In the following, we suppose that $e=1$ to simplify the exposition. However, it is easy to extend the case $0<e<1$, see Ref. [5] for details.

Enlightened by the work done by Yang *et al.*,[4,5] $T_\varepsilon(x,\omega)$ can be obtained into the series of the following form:

$$\begin{aligned} T_\varepsilon(x,\omega) &= T_0(x)+\varepsilon N_{\alpha_1}(y,\omega^s)\frac{\partial T_0(x)}{\partial x_{\alpha_1}}\\ &\quad+\varepsilon^2\left[N_{\alpha_1\alpha_2}(y,\omega^s)\frac{\partial^2 T_0(x)}{\partial x_{\alpha_1}\partial x_{\alpha_2}}\right.\\ &\quad\left.+C_{\alpha_1}(y,\omega^s)T_0^3(x)\frac{\partial T_0(x)}{\partial x_{\alpha_1}}\right],\\ &\quad x\in\Omega^{\varepsilon},\quad y\in Y^{*s}, \end{aligned} \tag{2}$$

where $T_0(x)$ is the homogenized solution, which reflects the macroscopic behaviors of the whole structure, $N_{\alpha_1}(y,\omega^s)$, $N_{\alpha_1\alpha_2}(y,\omega^s)$, and $C_{\alpha_1}(y,\omega^s)$ $(\alpha_1,\ \alpha_2=1,2,3)$ $(s=1,2,3,\ldots)$ denote local solutions, and $\omega=\{\omega^s,\ x\in\varepsilon Y^{*s}\subset\Omega^{\varepsilon}\}$.

For any fixed sample ω^s $(s=1,2,3,\ldots)$, $N_{\alpha_1}(y,\omega^s)$ $(\alpha_1=1,2,3)$ is the solution of the following boundary problem:

$$\begin{cases} \dfrac{\partial}{\partial y_i}\left[k_{ij}(y,\omega^s)\dfrac{\partial N_{\alpha_1}(y,\omega^s)}{\partial y_j}\right]=-\dfrac{\partial k_{i\alpha_1}(y,\omega^s)}{\partial y_i}, & \text{in } Y^{*s},\\ -\nu_i\left[k_{ij}(y,\omega^s)\dfrac{\partial N_{\alpha_1}(y,\omega^s)}{\partial y_j}+k_{i\alpha_1}(y,\omega^s)\right]=0, & y\in\Gamma,\\ N_{\alpha_1}(y,\omega^s)=0, & y\in\partial Y^s, \end{cases} \tag{3}$$

where Γ denotes the part domain that the surfaces of the cavities comprised in Y^s, such that $\Gamma=\bigcup_{n=1}^{N}\Gamma_n^c$, and N is the number of cavities contained in the unit cell Y^s; Y^{*s} is the solid part of Y^s. By the Lax–Milgram theorem, Poincare's inequality and supposition (ii), problem (3) has one unique solution.

Referring to Refs. [5], [18], and [19], for any fixed sample ω^s $(s=1,2,3,\ldots)$, the homogeneous parameters are defined as

$$\begin{aligned} \hat{k}_{ij}(\omega^s) &= \frac{1}{|Y^{*s}|}\int_{Y^{*s}}\left(k_{ip}(y,\omega^s)\frac{\partial N_j(y,\omega^s)}{\partial y_p}\right.\\ &\quad\left.+k_{ij}(y,\omega^s)\right)\mathrm{d}y. \end{aligned} \tag{4}$$

By applying Kolmogorov's classical strong law of large number (see Refs. [5] and [18]–[21]), we can evaluate the expected homogenized coefficients, which are equivalent to the thermal conductivity coefficients $\bar{\bar{k}}_{ij}$ as follows:

$$\bar{\bar{k}}_{ij}=\lim_{M\to\infty}\frac{\sum_{s=1}^{M}\dfrac{|Y^{*s}|\,\hat{k}_{ij}(\omega^s)}{|Y^s|}}{M}, \tag{5}$$

and define

$$\bar{k}_{ij}=\lim_{M\to\infty}\frac{\sum_{s=1}^{M}\hat{k}_{ij}(\omega^s)}{M}, \tag{6}$$

where M is the maximum number of samples. Similarly to the proof in Ref. [13], it is proved that $\bar{k}_{ij}$ $(i,j=1,2,3)$ are symmetrical and positive defined.

After the expected homogenized coefficients obtained from the unit cell Y^{*s}, the homogenized equations can be obtained as follows:

$$\begin{cases} -\dfrac{\partial}{\partial x_i}\left(\bar{k}_{ij}\dfrac{\partial T_0(x)}{\partial x_j}\right)=f(x), & \text{in } \Omega,\\ T_0(x)=\bar{T}(x), & \text{on } \Gamma_1,\\ \nu_i\bar{k}_{ij}\dfrac{\partial T_0(x)}{\partial x_j}=0, & \text{on } \Gamma_2, \end{cases} \tag{7}$$

where $T_0(x)$ is called the expected homogenized solution on Ω. By the Lax–Milgram theorem and Poincare's inequality, the homogenized problem (7) has a unique solution.

By the constructing way analogous to determining $N_{\alpha_1}(y,\omega^s)$, $N_{\alpha_1\alpha_2}(y,\omega^s)$ $(\alpha_1,\ \alpha_2 = 1,2,3)$ is the solution of the boundary value problem as follows:

$$\begin{cases} \dfrac{\partial}{\partial y_i}\left[k_{ij}(y,\omega^s)\dfrac{\partial N_{\alpha_1\alpha_2}(y,\omega^s)}{\partial y_j}\right] \\ = \bar{k}_{\alpha_1\alpha_2} - \dfrac{\partial}{\partial y_i}\left[k_{i\alpha_2}(y,\omega^s)N_{\alpha_1}(y,\omega^s)\right] \\ -k_{\alpha_1\alpha_2}(y,\omega^s) - k_{\alpha_2 j}(y,\omega^s)\dfrac{\partial N_{\alpha_1}(y,\omega^s)}{\partial y_j}, & \text{in } Y^{*s}, \\ -v_i\left[k_{ij}(y,\omega^s)\dfrac{\partial N_{\alpha_1\alpha_2}(y,\omega^s)}{\partial y_j}\right. \\ \left. +k_{i\alpha_2}(y,\omega^s)N_{\alpha_1}(y,\omega^s)\right] = 0, & y\in\Gamma, \\ N_{\alpha_1\alpha_2}(y,\omega^s) = 0, & y\in\partial Y^s. \end{cases} \tag{8}$$

Here, $C_{\alpha_1}(y,\omega^s)$ $(\alpha_1 = 1,2,3)$ is the solution of the following boundary value problem:

$$\begin{cases} \dfrac{\partial}{\partial y_i}\left[k_{ij}(y,\omega^s)\dfrac{\partial C_{\alpha_1}(y,\omega^s)}{\partial y_j}\right] = 0, & \text{in } Y^{*s}, \\ -v_i k_{ij}(y,\omega^s)\dfrac{\partial C_{\alpha_1}(y,\omega^s)}{\partial y_j} \\ = 4\sigma(N_{\alpha_1}(y,\omega^s) - \int_{\Gamma^c} N_{\alpha_1}(l,\omega^s)F(y,l)\mathrm{d}l), & y\in\Gamma, \\ C_{\alpha_1}(y,\omega^s) = 0, & y\in\partial Y^s, \end{cases} \tag{9}$$

where $l = z/\varepsilon$, z denotes the macroscopic coordinate and l is the local coordinate of 1-normalized cell.

Remark 2 Similarly to the proof in Refs. [4] and [5] under suppositions (I)–(IV) and (ii), the existence and uniqueness of Eqs. (8) and (9) can be easily established.

Now, we can define the two-scale approximate solutions of problem (1) given by

$$\begin{aligned} T_1^\varepsilon(x,\omega) &= T_0(x) + \varepsilon N_{\alpha_1}(y,\omega^s)\frac{\partial T_0(x)}{\partial x_{\alpha_1}}, \\ T_2^\varepsilon(x,\omega) &= T_0(x) + \varepsilon N_{\alpha_1}(y,\omega^s)\frac{\partial T_0(x)}{\partial x_{\alpha_1}} \\ &\quad + \varepsilon^2\left[N_{\alpha_1\alpha_2}(y,\omega^s)\frac{\partial^2 T_0^3}{\partial x_{\alpha_1}\partial x_{\alpha_2}}\right. \\ &\quad \left. + C_{\alpha_1}(y,\omega^s)T_0^3(x)\frac{\partial T_0(x)}{\partial x_{\alpha_1}}\right], \end{aligned} \tag{10}$$

where $T_1^\varepsilon(x,\omega)$ and $T_2^\varepsilon(x,\omega)$ represent the statistical first-order and the second-order two-scale approximate solutions, respectively.

For any fixed sample ω^s, to compare $T_1^\varepsilon(x,\omega)$ with the original solution (1), we substitute $T_\varepsilon(x,\omega) - T_1^\varepsilon(x,\omega)$ into Eq. (1), and have

$$\begin{aligned} & L_\varepsilon\left(T_\varepsilon(x,\omega) - T_1^\varepsilon(x,\omega)\right) \\ &= f(x) + k_{ij}(y,\omega^\varepsilon)\frac{\partial N_{\alpha_1}(y,\omega^\varepsilon)}{\partial y_j}\frac{\partial^2 T_0}{\partial x_i\partial x_{\alpha_1}} \\ &\quad + \frac{\partial}{\partial y_i}\left[k_{ij}(y,\omega^\varepsilon)N_{\alpha_1}(y,\omega^\varepsilon)\right]\frac{\partial^2 T_0}{\partial x_j\partial x_{\alpha_1}} \\ &\quad + k_{ij}(y,\omega^\varepsilon)\frac{\partial^2 T_0}{\partial x_i\partial x_j} \\ &\quad + \varepsilon k_{ij}(y,\omega^\varepsilon)\frac{\partial^2}{\partial x_i\partial x_j}\left(N_{\alpha_1}(y,\omega^\varepsilon)\frac{\partial T_0}{\partial x_{\alpha_1}}\right), \end{aligned}$$

where

$$L_\varepsilon = -\frac{\partial}{\partial x_i}\left(k_{ij}^\varepsilon(x,\omega)\frac{\partial}{\partial x_j}\right)$$

and $T_0 = T_0(x)$. It is not difficult to see that the residual is the order of $O(1)$. While, in the practical engineering computation, ε is a fixed smaller constant rather than tending to zero. The error $O(1)$ is not accepted for the engineers who want to capture the local behavior inside materials, so the first order solution is not adopted in engineering computation.

In addition, by taking $T_\varepsilon(x,\omega) - T_2^\varepsilon(x,\omega)$ into Eq. (1) and considering the homogenized equation (7), the following results can be obtained:

$$\begin{aligned} & L_\varepsilon\left(T_\varepsilon(x,\omega) - T_2^\varepsilon(x,\omega)\right) \\ &= -\frac{\partial}{\partial x_i}\left\{k_{ij}^\varepsilon(x,\omega)\frac{\partial T_\varepsilon(x,\omega)}{\partial x_j}\right. \\ &\quad + \frac{\partial}{\partial x_i}\left(k_{ij}^\varepsilon(x,\omega)\frac{\partial}{\partial x_j}\left[T_0 + \varepsilon N_{\alpha_1}(y,\omega^\varepsilon)\frac{\partial T_0}{\partial x_{\alpha_1}}\right.\right. \\ &\quad \left.\left. + \varepsilon^2\left(N_{\alpha_1\alpha_2}(y,\omega^\varepsilon)\frac{\partial^2 T_0}{\partial x_{\alpha_1}\partial x_{\alpha_2}} + C_{\alpha_1}(y,\omega^\varepsilon)T_0^3\frac{\partial T_0}{\partial x_{\alpha_1}}\right)\right]\right\} \\ &= -\frac{\partial}{\partial x_i}\left(\bar{k}_{ij}\frac{\partial T_0}{\partial x_j}\right) \\ &\quad + \left(\frac{\partial}{\partial x_i} + \frac{1}{\varepsilon}\frac{\partial}{\partial y_i}\right)\left\{k_{ij}^\varepsilon(x,\omega)\left(\frac{\partial}{\partial x_j} + \frac{1}{\varepsilon}\frac{\partial}{\partial y_j}\right)\right. \\ &\quad \times\left[T_0 + \varepsilon N_{\alpha_1}(y,\omega^\varepsilon)\frac{\partial T_0}{\partial x_{\alpha_1}}\right. \\ &\quad \left.\left. + \varepsilon^2\left(N_{\alpha_1\alpha_2}(y,\omega^\varepsilon)\frac{\partial^2 T_0}{\partial x_{\alpha_1}\partial x_{\alpha_2}} + C_{\alpha_1}(y,\omega^\varepsilon)T_0^3\frac{\partial T_0}{\partial x_{\alpha_1}}\right)\right]\right\} \\ &= \varepsilon^{-1}\left[\frac{\partial}{\partial y_i}\left(k_{ij}(y,\omega^s)\frac{\partial N_{\alpha_1}(y,\omega^s)}{\partial y_j}\right) + \frac{\partial k_{i\alpha_1}(y,\omega^s)}{\partial y_i}\right]\frac{\partial T_0}{\partial x_{\alpha_1}} \\ &\quad \times\left[\frac{\partial}{\partial y_i}\left(k_{ij}(y,\omega^s)\frac{\partial N_{\alpha_1\alpha_2}(y,\omega^s)}{\partial y_j}\right)\right. \\ &\quad + \frac{\partial}{\partial y_i}\left(k_{i\alpha_2}(y,\omega^s)N_{\alpha_1}(y,\omega^s)\right) \\ &\quad \left. + k_{\alpha_1\alpha_2}(y,\omega^s) + k_{\alpha_2 j}(y,\omega^s)\frac{\partial N_{\alpha_1}(y,\omega^s)}{\partial y_j} - \bar{k}_{\alpha_1\alpha_2}\right]\frac{\partial^2 T_0^3}{\partial x_{\alpha_1}\partial x_{\alpha_2}} \\ &\quad + \frac{\partial}{\partial y_i}\left[k_{ij}(y,\omega^s)\frac{\partial C_{\alpha_1}(y,\omega^s)}{\partial y_j}\right]T_0^3\frac{\partial T_0}{\partial x_{\alpha_1}} \\ &\quad + \varepsilon F_0 + \varepsilon^2\frac{\partial}{\partial x_i}F_i, \end{aligned} \tag{11}$$

where

$$F_0 = k_{ij}(y,\omega^\varepsilon)N_{\alpha_1}(y,\omega^\varepsilon)\frac{\partial^3 T_0}{\partial x_i\partial x_j\partial x_{\alpha_1}}$$

$$
\begin{aligned}
&+k_{ij}(y,\omega^{\varepsilon})\frac{\partial N_{\alpha_1\alpha_2}(y,\omega^{\varepsilon})}{\partial y_j}\frac{\partial^3 T_0}{\partial x_i\partial x_{\alpha_1}\partial x_{\alpha_2}}\\
&+\frac{\partial}{\partial y_i}\left[k_{ij}(y,\omega^{\varepsilon})N_{\alpha_1\alpha_2}(y,\omega^{\varepsilon})\right]\frac{\partial^3 T_0}{\partial x_j\partial x_{\alpha_1}\partial x_{\alpha_2}}\\
&+k_{ij}(y,\omega^{\varepsilon})\frac{\partial C_{\alpha_1}(y,\omega^{\varepsilon})}{\partial y_j}\frac{\partial}{\partial x_i}\left(T_0^3\frac{\partial T_0}{\partial x_{\alpha_1}}\right)\\
&+\frac{\partial}{\partial y_i}\left[k_{ij}(y,\omega^{\varepsilon})C_{\alpha_1}(y,\omega^{\varepsilon})\right]\frac{\partial}{\partial x_j}\left(T_0^3\frac{\partial T_0}{\partial x_{\alpha_1}}\right)\\
&+\varepsilon k_{ij}(y,\omega^{\varepsilon})N_{\alpha_1\alpha_2}(y,\omega^{\varepsilon})\frac{\partial^4 T_0}{\partial x_i\partial x_j\partial x_{\alpha_1}\partial x_{\alpha_2}},\\
F_i \;=\; & k_{ij}(y,\omega^{\varepsilon})C_{\alpha_1}(y,\omega^{\varepsilon})\frac{\partial}{\partial x_j}\left(T_0^3\frac{\partial T_0}{\partial x_{\alpha_1}}\right). \qquad (12)
\end{aligned}
$$

By virtue of Eq. (12) and the definitions of $N_{\alpha_1}(y,\omega^s)$, $N_{\alpha_1\alpha_2}(y,\omega^s)$, and $C_{\alpha_1}(y,\omega^s)$ $(\alpha_1,\ \alpha_2=1,2,3)$ $(s=1,2,3,\ldots)$ given by Eqs. (3), (8), and (9), the first term, the second term, and the third term on the right side of Eq. (11) are equal to zero. Note that the residual of Eq. (11) is the order of $O(\varepsilon)$. Obviously, the second-order solution is equivalent to the solution of the original problem in $O(\varepsilon)$-order pointwise sense. It is the main reason that we consider the second-order expansions in this paper.

Summing up, one obtains the following theorem.

Theorem 1 $\Omega^{\varepsilon}\subset R^3$ is a bounded Lipschitz convex domain. For any sample $\omega^s\in P$ $(s=1,2,3,\ldots)$, the heat conduction problem with radiation boundary condition (1) for porous materials with random distribution formally has an SSOTS asymptotic expansion as follows:

$$
\begin{aligned}
T_{\varepsilon}(x,\omega) \;=\; & T_0(x)+\varepsilon N_{\alpha_1}(y,\omega^s)\frac{\partial T_0(x)}{\partial x_{\alpha_1}}\\
&+\varepsilon^2\left[N_{\alpha_1\alpha_2}(y,\omega^s)\frac{\partial^2 T_0(x)}{\partial x_{\alpha_1}\partial x_{\alpha_2}}\right.\\
&\left.+C_{\alpha_1}(y,\omega^s)T_0^3(x)\frac{\partial T_0(x)}{\partial x_{\alpha_1}}\right]+\varepsilon^3 P(x,y,\omega^s),\\
&x\in\Omega^{\varepsilon},y\in Y^{*s}, \qquad (13)
\end{aligned}
$$

where $T_0(x)$ is the solution of homogenized problem (7) with the parameters (6). $N_{\alpha_1}(y,\omega^s)$, $N_{\alpha_1\alpha_2}(y,\omega^s)$, and $C_{\alpha_1}(y,\omega^s)$ $(\alpha_1,\ \alpha_2=1,2,3)$ $(s=1,2,3,\ldots)$ denote the local solutions satisfying Eqs. (3), (8), and (9), respectively. The $P(x,y,\omega^s)$ is the asymptotic expansion function depending on the two-scale variables x and y, and $\omega=\{\omega^s\ ,\ x\in\varepsilon Y^{*s}\subset\Omega^{\varepsilon}\}$.

4. Numerical experiments and discussion

In this section, some heat transfer examples are given to verify the validity and feasibility of the statistical two-scale method developed in this work.

4.1. Algorithm validation

A macrostructure Ω^{ε}, which is a union of entire periodic cells as illustrated in Fig. 2(a), is chosen, and the unit cell is shown in Fig. 2(b). The boundary temperatures in the x_3 direction are set as $\bar{T}_1(x)=0$ K, $\bar{T}_2(x)=0$ K, respectively. $\sigma=5.669996\times10^{-8}$ W·m^{-2}·K^{-4}, and the radius of the cavity in Y^* is 0.25. $k_{ij}=10\delta_{ij}$ W·m^{-1}·K^{-1}, $f(x)=10^5$ J·m^{-3}·s^{-1}, where δ_{ij} $(i,j=1,2,3)$ is the Kronecker delta.

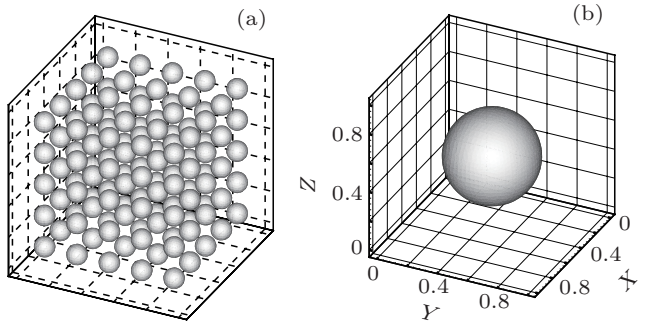


Fig. 2. (a) Domain $\Omega^{\varepsilon}=[0,0.25]^3$; (b) unit cell $Y^*=[0,1]^3$.

As the theoretical solution of the coupled heat transfer problem is difficult to find, we have to replace $T_{\varepsilon}(x,t)$ by the FE solution T_FE with a very fine mesh. We employ the linear tetrahedral elements to compute the coupled problem of Eq. (1) by fine meshes, and solve the corresponding homogenized equation by a coarse mesh. The numbers of tetrahedrons and nodes are shown in Table 1.

Table 1. Computational cost for comparison.

	Original equation	Unit cell	Homogenized equation
Elements	736815	5817	93750
Nodes	137431	1351	17576

It should be emphasized that $T_0(x,\omega)$ is the approximate solution of the homogenized equation (7), $T_1^{\varepsilon}(x,\omega)$ and $T_2^{\varepsilon}(x,\omega)$ are the first-order and the second-order two-scale approximate solutions based on Eq. (10).

Figures 3(a)–3(d) illustrate the computational results for $T_0(x,\omega)$, $T_1^{\varepsilon}(x,\omega)$, $T_2^{\varepsilon}(x,\omega)$, and T_FE at the intersection $x_3=0.15$.

Figure 4(a) and 4(b) show the computational results for temperature gradient $\partial T_{\varepsilon}(x,\omega)/\partial x_1$, $\partial T_{\varepsilon}(x,\omega)/\partial x_2$ along the lines of $x_1=x_2$, $x_3=0.15$.

From the computational results given in Figs. 3 and 4, it follows that the homogenized solution and the first-order solution are not effective to catch the local behavior of the solution for the coupled problems. However, the computational results displayed clearly verify that the second-order two-scale solution gives a more accurate numerical solution. Obviously, it can be concluded that the two-scale model proposed in this paper is sufficiently correct for computing the heat conduction problem with radiation boundary condition.

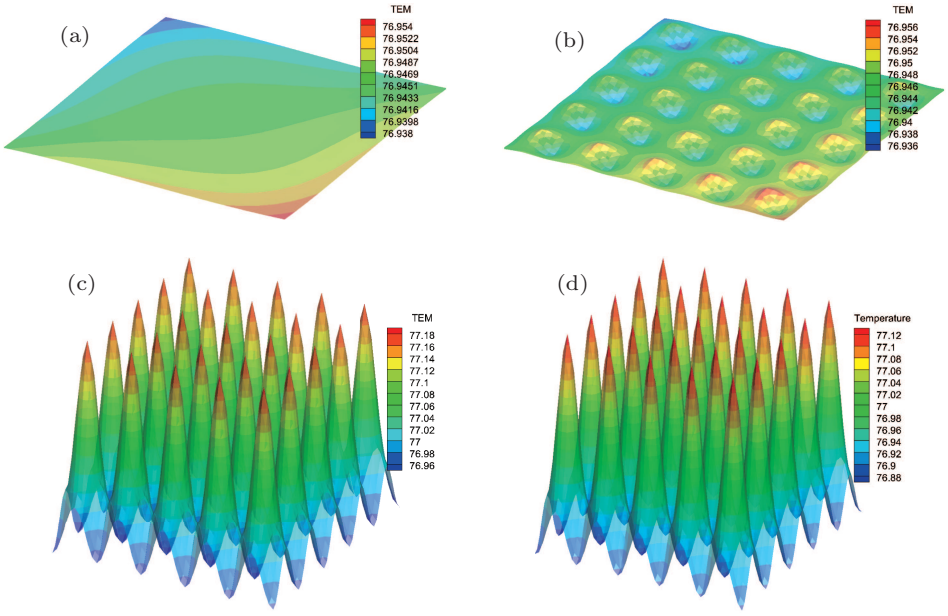


Fig. 3. (color online) The temperature fields in the cross section $x_3 = 0.15$; (a) $T_0(x,\omega)$; (b) $T_1^{\varepsilon}(x,\omega)$; (c) $T_2^{\varepsilon}(x,\omega)$; (d) T_FE.

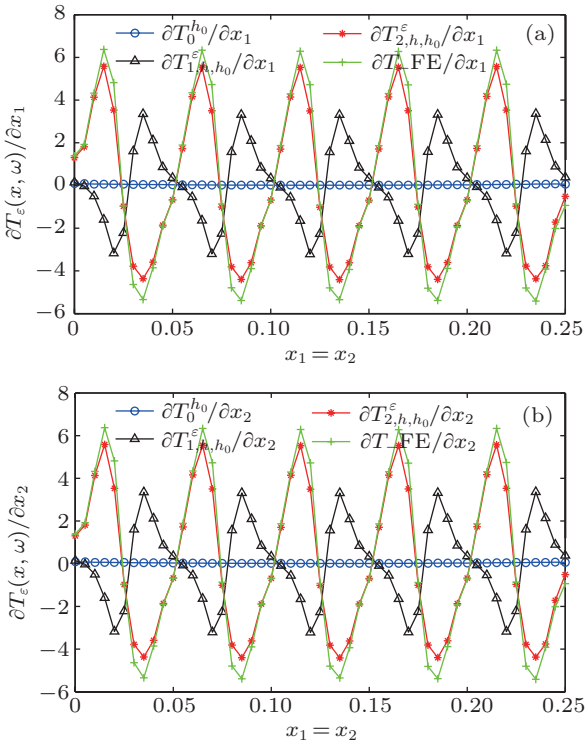


Fig. 4. (color online) (a) $\partial T_\varepsilon(x,\omega)/\partial x_1$; (b) $\partial T_\varepsilon(x,\omega)/\partial x_2$ along the lines of $x_1 = x_2$, x_3=0.15.

In addition, from Table 1, it can be seen that the mesh numbers of the second-order two-scale approximate solution previously are much less than that of the FE solution with fine meshes, and the computational time is also much less than that of the FE solution, especially for small ε. Consequently, the second-order two-scale method is of great importance in engineering computations owing to the importance of saving computer memory and CPU time. Actually, both the two-scale method and the direct finite element method are performed on the same computer (which has memory of 512 GB and 16 processors with CPU = 2.67 GHz). Considering the two-scale method previously, which is very cheap to solve the simulation (it takes about 1 s to finish solving the cell problems, and homogenized problem about 8 s for one iteration). On the other hand, the direct finite element simulation needs 620 s to compute the heat transfer problem for one iteration in the same examples since it requires very fine meshes.

4.2. Thermal properties of randomly distributed porous materials

In order to investigate the thermal performance of the porous materials, we consider three different types of microscopic distributions: spherical pores subject to a uniformly stochastic distribution in a ε-cell; spherical pores subject to a normal distribution around the centric point of ε-cell; orientations of ellipsoidal pores, whose long axes are two times that of the middle axes and short axes, which are subjected to normal distribution along the x_1 axis, and subjected to uniformly stochastic distribution in ε-cell. The distributions of orientations, shapes, and locations of pores on macroscopic properties of the materials are investigated by the SSOTS method, and due to pores random dispersion, the numerical results of different samples will vary even for the same distribution models of pores. Therefore, to obtain more accurate prediction values, a number of samples are required.

Figure 5 depicts the geometry structure of the plate studied with the length of 10 mm, width of 10 mm, and thickness of 5 mm, respectively. The temperatures in the x_3 direction are set as $\bar{T}_1(x)$, $\bar{T}_2(x)$ on the Γ_1. The radii are both taken as 0.04 for the pores subjected to a uniform distribution and pores subjected to a normal distribution. As the orientations of spherical

pores are in a normal distribution, the sizes of their long axes are taken as 0.1, while middle axes and short axes are both 0.05.

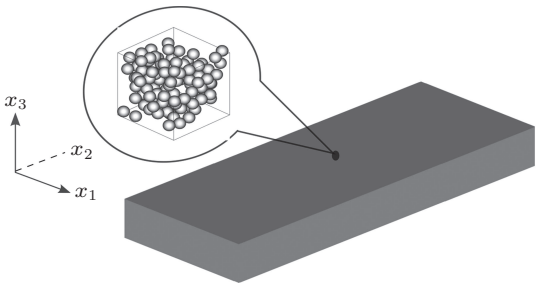


Fig. 5. Schematic of porous material plate.

4.2.1. Microstructure effect of porous materials on the effect of thermal conductivity parameters

The thermal conductivity of ceramics is[5,28] 4.41 $\mathrm{W{\cdot}m^{-1}{\cdot}K^{-1}}$. The internal heat source $f(x)$ is taken as zero and $\bar{T}_1(x) = 100$ K, $\bar{T}_2(x) = 1000$ K. At this level, the homogenized parameters for the effective thermal conductivity $\bar{\bar{k}}_{ij}$ $(i, j = 1,2,3)$ are computed for different samples and compared to corresponding measurements obtained from different numerical models.

The homogenized thermal conductivity coefficients $\bar{\bar{k}}_{ij}$ $(i, j = 1,2,3)$ in a unit statistic screen for some samples are displayed in Table 2 as a volume fraction of 20% with a uniform distribution of pores. Then, the expected homogenized parameters are computed by the procedure of the SSOTS algorithms previously.

Table 2. The homogenized coefficients $\{\bar{\bar{k}}_{ij}\}$ $(\mathrm{W{\cdot}m^{-1}{\cdot}K^{-1}})$ for different samples as volume fractions for 20% with a uniform distribution of pores.

No.	$\bar{\bar{k}}_{11}$	$\bar{\bar{k}}_{12}$	$\bar{\bar{k}}_{13}$	$\bar{\bar{k}}_{22}$	$\bar{\bar{k}}_{23}$	$\bar{\bar{k}}_{33}$
5	3.3434216	0.00060946119	0.00010964318	3.3346926	0.0021270333	3.330518
10	3.3441258	0.0008014546	0.0012766311	3.3355239	0.0025972413	3.3301634
20	3.3429517	0.0016516943	0.0018878259	3.3356398	0.0010416966	3.3374127
30	3.342679	0.00094525486	0.0013600499	3.3355809	0.00056567049	3.3334383
40	3.3428481	$-7.4151472\times^{-5}$	0.0013087926	3.3357914	0.0016423277	3.3337254
50	3.3426518	-4.4637085×10^{-5}	0.00086218149	3.3355769	0.00095091942	3.3333437

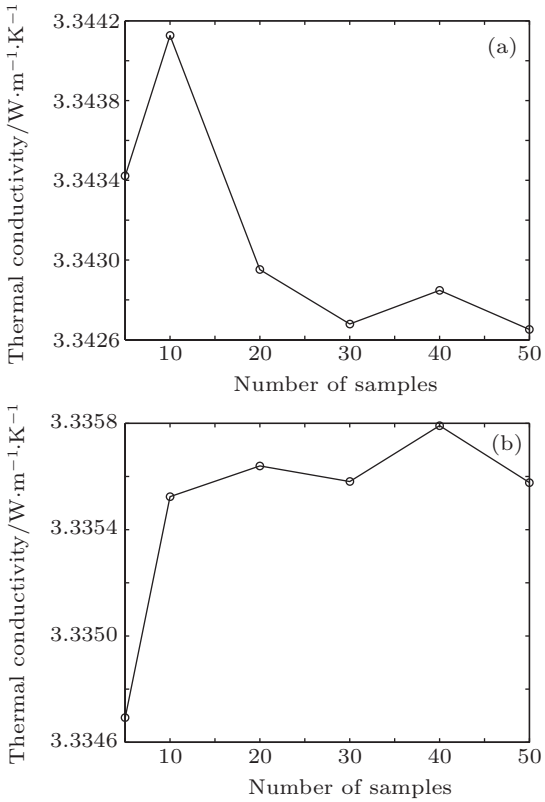


Fig. 6. Effective thermal conductivity k_{11} (a) and k_{22} (b) for different sample numbers.

Figure 6 with the expected homogenized thermal conductivity in different samples illustrates the convergence of the expected homogenized parameters for volume fractions of 20% with a uniform distribution of pores. Statistically, depicted in Fig. 6, the different samples should have different prediction results. However, as the increasing number of samples with the same microstructure, the mathematical expectation of the computational results should converge. As a result, the scatter of data decreases with the increase of the number of samples, shown in Fig. 6. Thus, 50 samples are chosen in this work to avoid an unacceptable scatter of the computational results.

Figure 7 displays the obtained values of the material coefficients from the statistical two-scale method as well as other computed values. The expected thermal conductivity results obtained from the proposed two-scale model agree well with the generalized self-consistent method[24] and the Maxwell–Eucken model[25] for a uniform distribution of pores. However, the empirical method cannot give satisfactory results for an orientation-normal distribution of spherical pores. In addition, the computational results based on the statistical two-scale model give better approximations of the empirical results at lower porosity, as the volume fractions increase, the deviations of the results increase. Obviously, it can be found that the SSOTS model developed in this paper is sufficiently accurate for predicting the effective properties of the porous materials.

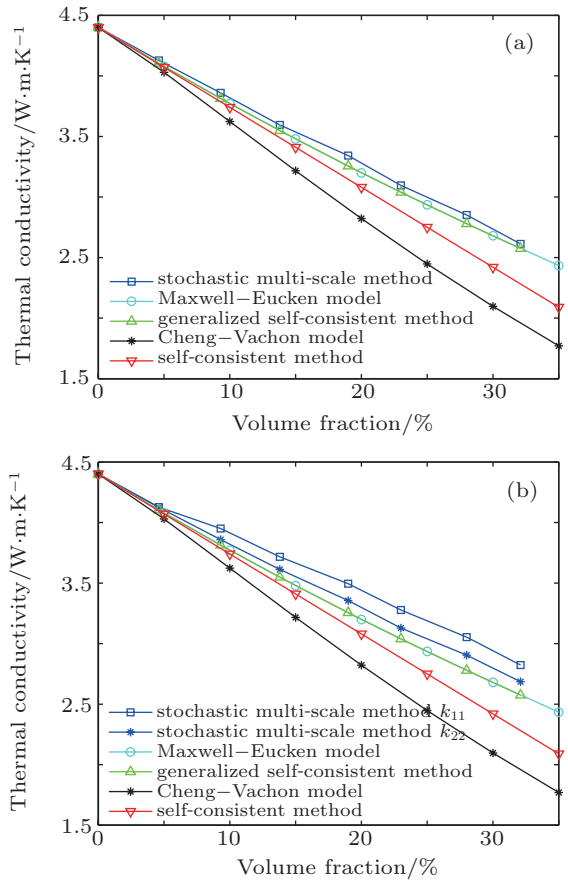


Fig. 7. (color online) Comparison of the thermal conductivity coefficients obtained from different numerical models (a) uniform distribution of pores; (b) orientation-normal distribution of spherical pores.

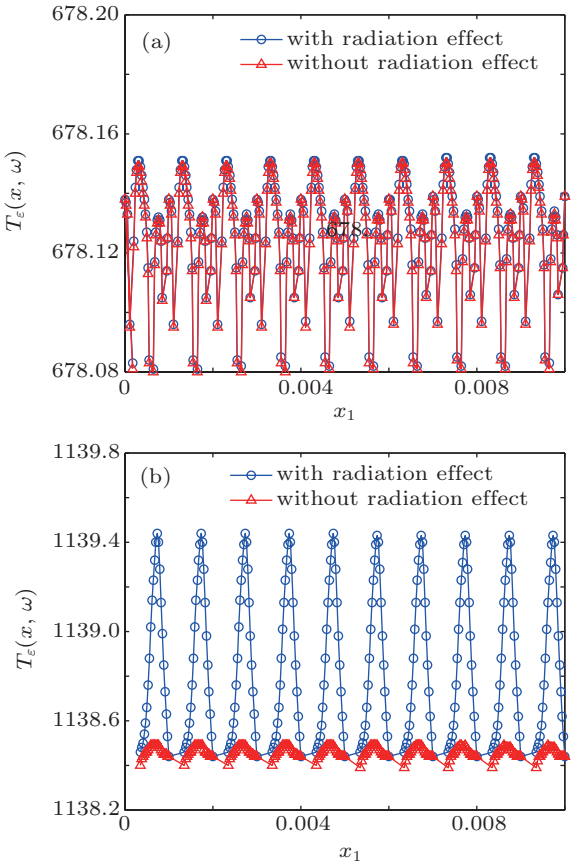


Fig. 8. (color online) The temperature field $T_2^\varepsilon(x,\omega)$ for boundary temperature (a) $\bar{T}_1(x) = 100$ K, $\bar{T}_2(x) = 1000$ K; (b) $\bar{T}_1(x) = 500$ K, $\bar{T}_2(x) = 1500$ K along the lines of $x_2 = 0.600167969$, $x_3 = 0.300844439$.

4.2.2. Radiation effect on macroscopic effective performance with different random distributions

Heat transfer properties of the porous materials not only depend on the material properties of the matrix phases but also on the volume fractions, location, orientation, spatial distribution, and radiation effect of the pores. Therefore, it is absolutely essential to investigate their influence on the macroscopic effective performance of the porous materials. The thermal conductivity of porous materials is 4.41 $\mathrm{W{\cdot}m^{-1}{\cdot}K^{-1}}$, and internal heat source $f(x)$ is set to 5000 $\mathrm{J{\cdot}m^{-3}{\cdot}s^{-1}}$. The volume fractions of the materials are limited to 20%, and pores are subjected to a uniformly stochastic distribution in a ε-cell.

Figure 8(a) illustrates the computational results of the temperature field $T_2^\varepsilon(x,\omega)$ for boundary temperature $\bar{T}_1(x) = 100$ K and $\bar{T}_2(x) = 1000$ K along the lines of $x_2 = 0.600167969$, $x_3 = 0.300844439$, whereas figure 8(b) displays the computational results of the temperature field $T_2^\varepsilon(x,\omega)$ for boundary temperature $\bar{T}_1(x) = 500$ K and $\bar{T}_2(x) = 1500$ K.

It can be clearly seen from the figures that the SSOTS method developed in this work is effective to catch the local microscopic behavior of the porous materials. In particular, the detailed information of the radiation effect on the surfaces of the cavities can be captured accurately by the developed two-scale model.

5. Conclusions

This paper discusses the SSOTS analysis and computation for the heat conduction problem with radiation boundary condition in porous materials. The second-order two-scale analysis formulae for the heat transfer problem are derived in detail. Furthermore, the correctness of this two-scale model and the effectiveness of the SSOTS method proposed in this paper are verified by comparing with FE methods with fine meshes. During the process of the numerical verification, it is well shown that the SSOTS method is accurate to numerically solve the heat conduction equation with radiation boundary condition.

The macroscopic thermal performance for the porous structures with varying probability distribution models, including volume fraction, orientation, and location distributions of pores, is displayed. By comparing the obtained results with empirical formulas in the references, the proposed statistical two-scale model is validated. Further, in order to study the influence of the volume fractions and the radiation effect of pores on the macroscopic properties of porous materials, different microstructure models of these materials are chosen for a comparison. Numerical results clearly show that the microscopic structure has a significant impact on the macroscopic thermal properties. Especially, these properties vary with the

probability model of random distributions of pores. Therefore, the SSOTS method and computation developed in this study can be used to predict the macroscopic thermal properties of the heat transfer problem and effectively catch the local behaviors caused by the microstructure inside the materials.

References

[1] Liu S T and Zhang Y C 2006 *Multidiscipline Modeling Mat. Str.* **2** 327
[2] Daryabeigi K 1999 37*th AIAA Aerospace Sciences Meeting and Exhibit*, January 11–14, 1999, Reno, NV
[3] Bakhvalov N S 1981 *Differ. Uraun.* **17** 1774
[4] Yang Z Q, Cui J Z, Nie Y F and Ma Q 2012 *CMES: Comp. Model. Eng.* **88** 419
[5] Yang Z Q, Cui J Z and Li Y Q 2013 *Int. J. Numer. Anal. Mod. Series B* **4** 151
[6] Allaire G and Ganaoui K El 2009 *Multiscale Model. Sim.* **7** 1148
[7] Ma Q and Cui J Z 2012 *Commun. Comput. Phys.* **14** 1027
[8] Amosov A A 2010 *J. Math. Sci.* **164** 309
[9] Amosov A A 2010 *J. Math. Sci.* **169** 1
[10] Tiihonen T 1997 *Math. Method. Appl. Sci.* **20** 47
[11] Qatanani N, Barham A and Heeh Q 2007 *Surv. Math. Appl.* **2** 43
[12] Yang Z Q, Cui J Z and Li B W 2014 *Chin. Phys. B* **23** 030203
[13] Oleinik O A, Shamaev A S and Yosifian G A 1992 *Mathematical Problems in Elasticity and Homogenization* (Amsterdam: North-Holland)
[14] Yang Z H, Chen Y, Yang Z Q and Ma Q 2014 *Chin. Phys. B* **23** 076501
[15] Weinan E and Engquist B 2003 *Commun. Math. Sci.* **1** 87
[16] Jikov V V, Kozlov S M and Oleinik O A 1994 *Homogenization of Differential Operators and Integral Functions* (Berlin: Springer)
[17] Dong H, Cui J Z, Nie Y F and Wu Y T 2015 *Chin. Phys. B* **24** 090204
[18] Li Y Y and Cui J Z 2005 *Compos. Sci. Technol.* **65** 1447
[19] Yu Y, Cui J Z and Han F 2008 *Compos. Sci. Technol.* **68** 2543
[20] Li Y Y and Long S Y 2009 *Appl. Math. Model.* **33** 3157
[21] He W M, Guan X F and Zhang X J 2011 *Int. J. Mod. Phys. B* **25** 143
[22] Mori T and Tanaka K 1973 *Acta Metall.* **21** 571
[23] Hill R 1965 *J. Mech. Phys. Solids* **13** 213
[24] Chou T W, Nomura S and Taya M 1980 *J. Compos. Mater.* **14** 178
[25] Hashin Z and Shtrikman S 1962 *J. Appl. Phys.* **33** 3125
[26] Yang Z Q, Cui J Z, Sun Y and Ge J R 2015 *Finite Elem. Anal. Des.* **102–103** 7
[27] Li Y Y 2009 *Math. Numer. Sin.* **31** 275 (in Chinese)
[28] Yan C H 2006 *Thermal Insulating Mechanism and Research on Thermal Insulating Efficiency of Thermal Insulations of Metallic Thermal Protection System* (Ph.D. Dissertation) (Harbin: Harbin Institute of Technology) (in Chinese)